Comb-Like Modal Dispersion Diagram in a Double-Wire Medium Slab

Solange V. Silva, Tiago A. Morgado, and Mário G. Silveirinha, *Fellow, IEEE*

(Invited Paper)

***Abstract*— We investigate the guided modes supported by a wire metamaterial slab formed by two mutually orthogonal and nonconnected sets of parallel metallic wires. It is demonstrated that the wire medium slab has a peculiar comb-like dispersion diagram. In the continuum approximation, the metamaterial supports a diverging number of guided mode branches that accumulate near the light line due to a strong hyperbolic response in the static limit. In a realistic system, the number of guided mode branches is finite and is determined by the density of wires. Remarkably, the guided modes may be characterized by a fast field variation along the transverse direction, which can be exploited to detect subwavelength particles or defects.**

***Index Terms*— Homogenization theory, metamaterials, spatial dispersion, surface waves, wire media.**

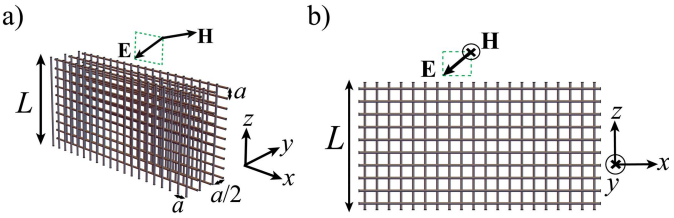

Fig. 1. Geometry of the crossed wire grid formed by two mutually orthogonal and nonconnected sets of metallic wires oriented along the x- and z-directions. The spacing between adjacent parallel wires is a, whereas the spacing between adjacent orthogonal wires is $a/2$. The thickness of the slab along the z-direction is L. (a) Perspective view and (b) top view.

I. Introduction

In recent years, there has been a great deal of interest in the physics and applications of wire metamaterials [1]. These artificial media are formed by long metallic rods arranged in various possible ways, ranging from simple periodic arrays of parallel wires [2]–[5] to more complex configurations with connected or nonconnected orthogonal sets of wires [1], [4], [6]–[8]. The unique geometry of the wire metamaterials (with long and thin inclusions), combined with the high optical contrast between the metallic wires and the dielectric background, gives rise to peculiar electromagnetic properties such as a strongly spatially dispersive (nonlocal) response [1], [5], [6], [9]–[11], extreme optical anisotropy [12], anomalously high density of photonic states [13]–[17], and low-loss broadband anomalous dispersion [18], [19]. These unusual properties lead to quite interesting applications, including near-field transport and manipulation [20]–[26], ultracompact waveguiding [27]–[29], negative refraction [30]–[33], near-field [34]–[36] and far-field [37], [38] superlensing, and the correction of chromatic aberrations [39]. Furthermore, wire metamaterials may boost the Cherenkov emission by charged particles [14], enhance the Purcell factor [15], the Casimir interactions [13], [16], [40], and the radiative near-field heat transfer [41].

Effective medium models enable the accurate and fast characterization of the electromagnetic response of wire metamaterials [5], [6], [9]–[11], [42]. In particular, homogenization methods have been used to analyze the guided modes supported by single-wire medium slabs [43]–[48] and double-wire medium slabs [27]–[29]. In the configurations studied in [27]–[29], the metallic wires are tilted by $\pm 45^\circ$ with respect to the interfaces. In contrast, here we characterize the transverse magnetic (TM) guided modes supported by a double-wire grid with one set of wires perpendicular to the interface with air and another set parallel to the interface [see Fig. 1]. Our analytical model is based on the transverse average (TA)-field approach introduced in [49] and [50], which enables taking into account explicitly the termination of the bulk structure. We demonstrate that in the continuum limit, the metamaterial slab supports a diverging (infinite) number of guided mode branches with dispersions that accumulate near the light line, with a comb-like structure. Interestingly, the guided modes that are weakly bounded to the wire metamaterial slab may exhibit a fast field variation along the transverse direction. We suggest that these waves may be useful to detect structural defects with subwavelength dimensions.

This article is organized as follows. In Section II, we briefly review the TA-field homogenization approach. In Section III, we discuss the properties of the fundamental TM bulk mode

Manuscript received May 4, 2019; revised October 10, 2019; accepted October 19, 2019. Date of publication November 4, 2019; date of current version March 3, 2020. This work was supported in part by the Institution of Engineering and Technology (IET) under the A F Harvey Research Prize 2018, in part by the Fundação para Ciência e a Tecnologia (FCT) under Project PTDC/EEI-TEL/4543/2014 and Project RETIOT, POCI-01-0145-FEDER-016432, and in part by the Instituto de Telecomunicações under Project UID/EEA/50008/2019. The work of S. V. Silva was supported by the Fundação para a Ciência e a Tecnologia (FCT/POPH) and the Fundo Social Europeu under the Ph.D. Fellowship under Grant SFRH/BD/105625/2015. The work of T. A. Morgado was supported by FCT under the CEEC Individual 2017 Contract as an Assistant Researcher (established with IT–Coimbra) with reference CT/N°004/2019-F00069. *(Corresponding author: Tiago Morgado.)*

S. V. Silva and T. A. Morgado are with the Instituto de Telecomunicações, University of Coimbra, 3030-290 Coimbra, Portugal, and also with the Department of Electrical Engineering, University of Coimbra, 3030-290 Coimbra, Portugal (e-mail: solange@co.it.pt; tmorgado@co.it.pt).

M. G. Silveirinha is with the Instituto Superior Técnico and Instituto de Telecomunicações, University of Lisbon, 1049-001 Lisbon, Portugal (e-mail: mario.silveirinha@co.it.pt).

Color versions of one or more of the figures in this article are available online at http://ieeexplore.ieee.org.

Digital Object Identifier 10.1109/TAP.2019.2950044

supported by the double-wire medium slab. In Section IV, we calculate the dispersion characteristic of the TM guided modes and compare the analytical results with full-wave simulations. Then, in Section V, we show that the guided modes can be used to detect subwavelength defects or imperfections. Finally, in Section VI, the conclusions are drawn.

In this article, we assume that the fields are monochromatic with a time variation $e^{j\omega t}$.

II. Homogenization Model

The wire metamaterial consists of a grid of nonconnected metallic wires with radius $r_{\rm w}$. The two mutually orthogonal sets of wires are oriented along the x- and z-directions, as illustrated in Fig. 1. The spacing between adjacent parallel wires is a, whereas the spacing between adjacent orthogonal wires is $a/2$. The wires are embedded in a standard dielectric with relative permittivity $\varepsilon_{\rm h}$.

In the long-wavelength regime ($\lambda \gg a$), the wire grid may be regarded as a continuum described by the relative dielectric function [6], [8], [51]

$$\bar{\varepsilon} = \varepsilon_{xx}\hat{\mathbf{x}}\otimes\hat{\mathbf{x}} + \varepsilon_{\rm h}\hat{\mathbf{y}}\otimes\hat{\mathbf{y}} + \varepsilon_{zz}\hat{\mathbf{z}}\otimes\hat{\mathbf{z}} \tag{1}$$

where $\hat{\mathbf{x}}$, $\hat{\mathbf{y}}$, and $\hat{\mathbf{z}}$ are the unit vectors along the coordinate axes. For ideal perfectly electrical conducting (PEC) thin wires ($r_{\rm w}/a \ll 1$), the relative permittivity components ε_{xx} and ε_{zz} are given by [6], [8], [51]

$$\varepsilon_{ii} = \varepsilon_{\rm h}\left(1 - \frac{\beta_{\rm p}^2}{\beta^2 - k_i^2}\right), \quad i = x, z \tag{2}$$

where $\beta_{\rm p}$ is the effective plasma wavenumber, $\beta = \sqrt{\varepsilon_{\rm h}}(\omega/c)$ is the wavenumber in the dielectric host, and c is the speed of light in vacuum. The parameter $\beta_{\rm p}$ uniquely depends on the geometrical properties of the structure [5] and satisfies

$$\beta_{\rm p} = \frac{1}{a}\sqrt{\frac{2\pi}{\ln\left(\frac{a}{2\pi r_{\rm w}}\right) + 0.5275}}. \tag{3}$$

In the usual approach, the bulk medium fields obtained from the effective dielectric function are used to characterize the wave propagation. However, for thin metamaterial slabs, the bulk medium fields may fail to accurately model the electromagnetic response near the interfaces, as shown in [50]. This happens in part because the electromagnetic response is sensitive to the termination plane, i.e., to the plane where the bulk material is truncated. To circumvent this problem, we rely on the TA-field approach introduced in [49] and [50]. In the TA-field approach, the microscopic fields are averaged only along the directions parallel to the interface (in the present problem, along the x- and y-directions). In contrast, the bulk medium fields are obtained by averaging the microscopic fields over the 3-D unit cell.

Interestingly, it was demonstrated in [50] that in some conditions, the TA fields can be written in terms of the bulk medium fields. In particular, for the considered wire grid, the TA fields associated with a plane wave of the bulk medium with electric field $\mathbf{E} = \mathbf{E}_{\rm av}e^{-j\mathbf{k}\cdot\mathbf{r}}$ and wave vector $\mathbf{k} = (k_x, k_y, k_z)$ are given by (for convenience, we use notations slightly different from the ones of [50])

$$\begin{aligned}\mathbf{E}_{\rm TA}(z; k_z) &= \beta^2\bar{\mathcal{G}}(z|z_x; \mathbf{k})e^{-jk_z z_x}\cdot\hat{\mathbf{x}}\hat{\mathbf{x}}\cdot(\varepsilon_{xx}-1)\mathbf{E}_{\rm av}e^{-j\mathbf{k}_{||}\cdot\mathbf{r}} \\ &\quad + \frac{1}{k^2-\beta^2}(\beta^2\mathbf{1} - \mathbf{k}\otimes\mathbf{k})e^{-jk_z z}\cdot\hat{\mathbf{z}}\hat{\mathbf{z}}\cdot(\varepsilon_{zz}-1)\,\mathbf{E}_{\rm av}e^{-j\mathbf{k}_{||}\cdot\mathbf{r}}\end{aligned} \tag{4a}$$

$$\mathbf{B}_{\rm TA} = \frac{1}{-j\omega}\left(-j\mathbf{k}_{||} + \frac{\partial}{\partial z}\hat{\mathbf{z}}\right)\times\mathbf{E}_{\rm TA} \tag{4b}$$

where $\mathbf{k}_{||} = (k_x, k_y, 0)$ is the transverse wave vector, $\mathbf{1}$ is the identity dyadic, and $z = z_x$ represents the z-coordinate of a generic plane of wires directed along the x-direction. The TA electric and induction fields are denoted by $\mathbf{E}_{\rm TA}$ and $\mathbf{B}_{\rm TA}$. The tensor $\bar{\mathcal{G}}$ is defined by [50]

$$\begin{aligned}\bar{\mathcal{G}}(z|z_x; \mathbf{k}) &= \left[\mathbf{1} + \frac{1}{\beta^2}\left(-j\mathbf{k}_{||} + \frac{\partial}{\partial z}\hat{\mathbf{z}}\right)\otimes\left(-j\mathbf{k}_{||} + \frac{\partial}{\partial z}\hat{\mathbf{z}}\right)\right]A(z - z_x; k_z)\end{aligned} \tag{5a}$$

$$A(z; k_z) = \frac{a}{2\gamma}\left[e^{-\gamma|z|} + \sum_{\pm}\frac{e^{\pm\gamma z}}{e^{(\gamma\pm jk_z)a} - 1}\right], \quad |z| < a/2. \tag{5b}$$

Here, $\gamma = \sqrt{k_{||}^2 - \beta^2}$ and the sum in (5b) is over two terms, one with the "+" sign and other with the "−" sign. The function $A(z; k_z)$ can be extended to arbitrary z as a Bloch wave with propagation constant k_z. For more details, a reader is referred to [50].

III. Isofrequency Contours of the Bulk Medium

We want to study the wave propagation in the xoz plane ($k_y = 0$) with magnetic field polarized along the y-direction [see Fig. 1]. The dispersion characteristic of the TM modes supported by the crossed wire grid is determined by [32]

$$\frac{k_x^2}{k^2 - \beta^2\varepsilon_{xx}} + \frac{k_z^2}{k^2 - \beta^2\varepsilon_{zz}} = 1 \tag{6}$$

which may be reduced to a polynomial equation of second degree in the variable k_z^2. This means that the crossed wire grid supports two independent TM plane wave modes with $\mathbf{H} = H_y\hat{\mathbf{y}}$ and propagation constants along z of the form $\pm k_z^{(1)}$ and $\pm k_z^{(2)}$. Thus, as compared to a standard dielectric, there is an additional TM wave. This property is a fingerprint of the strongly nonlocal response of the wire metamaterial [6], [8], [51]. It turns out that for long wavelengths, one of the TM waves is an evanescent wave ($\pm k_z^{(2)}$ is purely imaginary), and thereby there is a single propagating mode in the wire grid (with real-valued propagation constant $\pm k_z^{(1)}$). The (bulk) fields associated with a generic TM plane wave are of the form

$$\mathbf{H} = H_0 e^{-j\mathbf{k}\cdot\mathbf{r}}\hat{\mathbf{y}}, \quad \mathbf{E} = \frac{H_0}{\omega\varepsilon_0}\left(\frac{k_z}{\varepsilon_{xx}}\hat{\mathbf{x}} - \frac{k_x}{\varepsilon_{zz}}\hat{\mathbf{z}}\right)e^{-j\mathbf{k}\cdot\mathbf{r}}. \tag{7}$$

The isofrequency contours of the propagating TM mode supported by the unbounded wire grid are depicted in Fig. 2(a). The isofrequency contours consist of two hyperbolas with

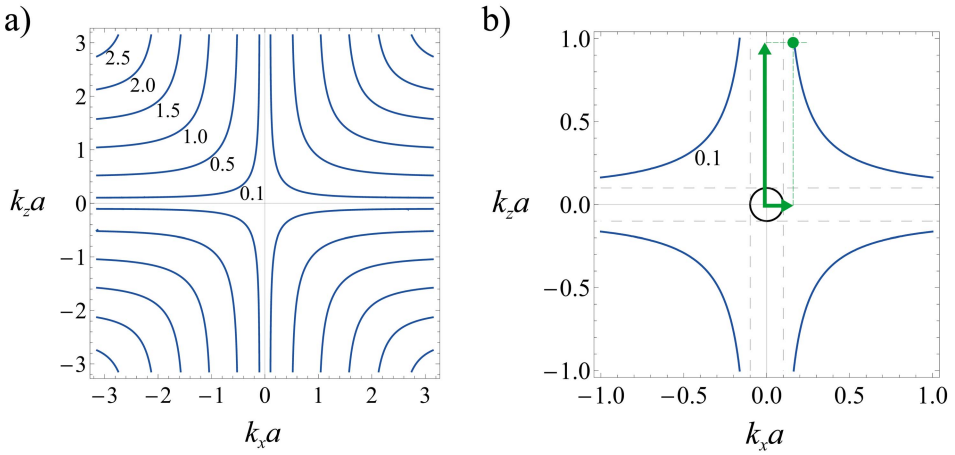

Fig. 2. (a) Isofrequency contours of the fundamental TM bulk mode for a metamaterial formed by wires standing in air. The wire radius is $r_w = 0.05a$. The text insets indicate the value of the normalized frequency $\omega a/c$. (b) Zoomed-in view of the first panel, together with the isofrequency contour of the air region (black solid line), for the normalized frequency $\omega a/c = 0.1$. The gray dashed lines represent the asymptotes of the hyperbolas. The green arrows represent the k_x and k_z components of the wave vector of a particular bulk mode with k_x slightly larger than ω/c.

asymptotes running along the x- and z-directions, i.e., the directions parallel to the two sets of wires. Curiously, the asymptotes correspond to the flat isofrequency contours of the TEM modes supported by each individual array of parallel wires [45], [52]. The shape of the isofrequency contours implies that the group velocity tends to be oriented along the wire directions.

Moreover, because of the hyperbolic nature of the isofrequency contours, the wire grid can support waves with rather large wave vectors. Interestingly, as $|k_x|$ approaches the host medium wavenumber ($|k_x| \to \beta + 0^+$), the corresponding $k_z \equiv k_z^{(1)}$ diverges to infinity [see Fig. 2(b)]. This suggests that a finite-thickness wire medium slab (truncated at $z = 0$ and $z = L$) may support weakly bounded guided modes with $|k_x|$ slightly larger than β. Specifically, if the host medium is air, the guided modes are expected to have dispersions near the light line and to be associated with fields that vary extremely fast along the z-direction. Note that heuristically the condition for the emergence of guided modes is that $k_z^{(1)} L \approx n\pi$ with $n = 1, 2, 3, \ldots$ an integer and $k_z^{(1)} = k_z^{(1)}(k_x, \omega)$ the positive real-valued solution of (6) with respect to k_z. Since $k_z^{(1)}$ has a divergent behavior as $|k_x| \to \omega/c$, it is obvious that $k_z^{(1)} L \approx n\pi$ can have an infinite number of solutions (each associated with a different n) with k_x slightly larger than ω/c. In other words, the continuum model predicts a diverging number of guided modes with dispersions piling up near the light line. In Section IV, this prediction is numerically verified.

IV. Dispersion Characteristic of the Guided Modes

The dispersion of the TM guided modes supported by the wire grid slab can be calculated in the usual way by expanding the electromagnetic fields in the air and wire grid regions in terms of plane waves. However, different from the standard homogenization approach, here the fields inside the wire metamaterial are written in terms of the TA fields, rather than in terms of the bulk fields. Specifically, for $0 < z < L$, one has

$$\mathbf{E}(z) = B_1^+ \mathbf{E}_{\mathrm{TA}}\left(z; k_z^{(1)}\right) + B_1^- \mathbf{E}_{\mathrm{TA}}\left(z; -k_z^{(1)}\right) + B_2^+ \mathbf{E}_{\mathrm{TA}}\left(z; k_z^{(2)}\right) + B_2^- \mathbf{E}_{\mathrm{TA}}\left(z; -k_z^{(2)}\right) \quad (8a)$$

$$\mathbf{H}(z) = B_1^+ \mathbf{H}_{\mathrm{TA}}\left(z; k_z^{(1)}\right) + B_1^- \mathbf{H}_{\mathrm{TA}}\left(z; -k_z^{(1)}\right) + B_2^+ \mathbf{H}_{\mathrm{TA}}\left(z; k_z^{(2)}\right) + B_2^- \mathbf{H}_{\mathrm{TA}}\left(z; -k_z^{(2)}\right) \quad (8b)$$

where $B_{1,2}^{\pm}$ are the complex amplitudes of the excited waves in the metamaterial and $\mathbf{E}_{\mathrm{TA}}(z; k)$ is found from the relevant bulk electric field in (7) using (4a) with $\mathbf{k}_{||} = k_x \hat{\mathbf{x}}$. Here, k_x is the wavenumber of the guided mode. Furthermore, $\mathbf{H}_{\mathrm{TA}} = \mathbf{B}_{\mathrm{TA}}/\mu_0$ is obtained from the corresponding $\mathbf{E}_{\mathrm{TA}}$ using (4b). Similarly, in the air regions it is possible to write

$$\mathbf{E} = \frac{1}{j\omega\varepsilon_0} e^{-jk_x x} \begin{cases} (\gamma_0 \hat{\mathbf{x}} - jk_x \hat{\mathbf{z}}) A_1 e^{-\gamma_0 (z-L)}, & z > L \\ (-\gamma_0 \hat{\mathbf{x}} - jk_x \hat{\mathbf{z}}) A_2 e^{+\gamma_0 z}, & z < 0 \end{cases} \quad (9a)$$

$$\mathbf{H} = \hat{\mathbf{y}} e^{-jk_x x} \begin{cases} A_1 e^{-\gamma_0 (z-L)}, & z > L \\ A_2 e^{+\gamma_0 z}, & z < 0 \end{cases} \quad (9b)$$

where $\gamma_0 = \sqrt{k_x^2 - \omega^2 \varepsilon_0 \mu_0}$ is the free-space propagation constant and $A_{1,2}$ are the complex amplitudes of the excited waves in the air regions.

At the interfaces with air ($z = 0$ and $z = L$), we enforce the continuity of the tangential components of the electromagnetic fields (H_y and E_x) and an additional boundary condition (ABC) [53], [54] that guarantees that the electric current flowing along the wires directed along z vanishes. When the host medium is the same in all the three regions of space, the ABC is equivalent to enforce that the normal component of the electric field (E_z) is continuous at the interfaces [54]. In this manner, we obtain a homogeneous 6×6 linear system. The dispersion of the TM guided modes is found by setting the determinant of the linear system equal to zero.

The calculated dispersion characteristic (ω versus k_x) of the TM guided modes for a wire grid with a fixed thickness L and

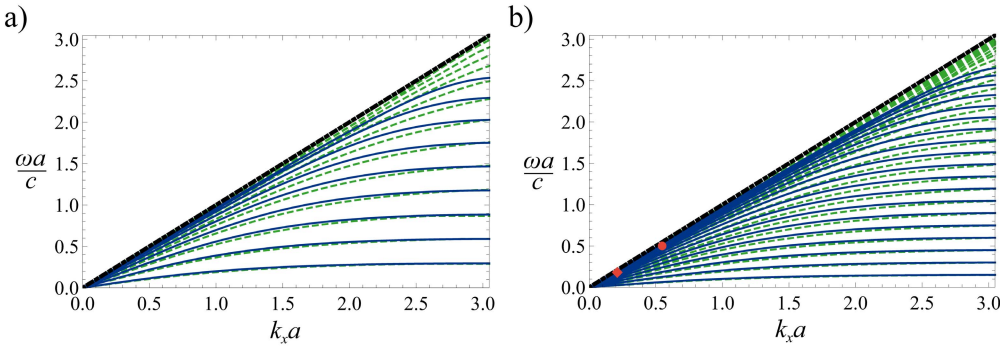

Fig. 3. Comb-like dispersion diagram of the TM guided modes supported by a metamaterial slab, for a fixed slab thickness L and different lattice period a. The radius of the wires is $r_w = 0.05a$. (a) $a = L/10$ and (b) $a = L/20$. The green dashed curves and the blue solid curves are obtained from the effective medium model and CST Microwave Studio simulations [55], respectively. The black dashed line represents the light line.

two different wire densities a/L is depicted in Fig. 3. As seen, the metamaterial slab has an intriguing dispersion diagram formed by a "comb" of guided mode branches that accumulate near the light line for low frequencies. The green dashed curves in Fig. 3 were obtained with the effective medium model, whereas the blue solid curves were calculated with the eigenmode solver of CST Microwave Studio [55] that takes into account the granularity of the metamaterial slab. The effective medium results concur well with the full-wave results, even for high frequencies and large wave vectors when the lattice constant becomes comparable to the wavelength and the homogenization is expected to become less accurate (the limit of the Brillouin zone).

The peculiar comb-like structure of the dispersion diagram is a consequence of the strongly hyperbolic response of the metamaterial near the static limit, as already discussed in Section III. Remarkably, within the effective medium framework—wherein the wire grid is regarded as an ideal electromagnetic continuum—the number of guided modes diverges to infinity [see green dashed curves in Fig. 3(a) and (b)]. In contrast, when the granularity of the metamaterial slab is taken into account, the number of guided modes becomes finite and depends on the wire density. Specifically, it turns out that the number of guided modes is exactly $N - 1$, where $N = L/a$ represents the number of unit cells along the z-direction. This feature is consistent with the fact that the structure is effectively a stack of N metallic sheets, if the wires oriented along z are ignored; that is, the structure may be roughly regarded as a transmission line formed by N independent conductors, which supports $N - 1$ independent transmission-line modes (quasi-TEM modes). Note that all the wires in the same $z =$ const. plane behave effectively as a single conductor.

In Fig. 4, we depict the transverse electromagnetic field distributions of the modes marked in Fig. 3(b) with the discrete red symbols. The results are calculated using both the effective medium model (solving the homogeneous system discussed in the beginning of Section IV) and the full-wave simulations [the guided mode is excited by a phased array of voltage generators placed along the z-axis, analogous to Fig. 5(b-ii)] [55]. As seen in Fig. 4(a-i) and (a-ii) and (b-ii), there is a reasonably good agreement between the two calculation methods, further demonstrating the validity of the TA-field approach. The agreement between the full-wave simulation

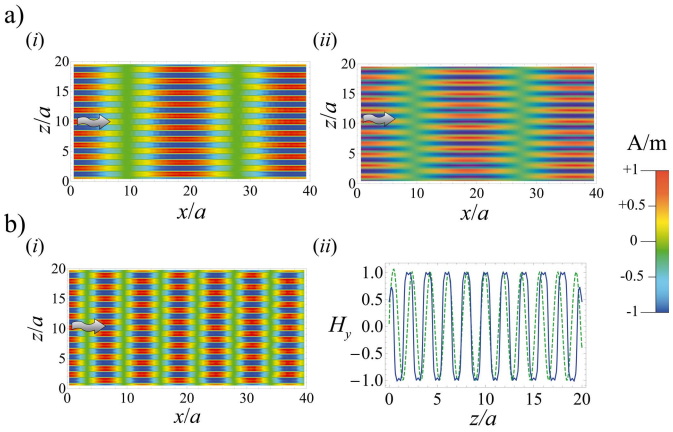

Fig. 4. (a) Magnetic field (H_y) distribution in the xoz-plane for the guided mode associated with the diamond-shaped red symbol in Fig. 3(b); the mode has $\omega a/c = 0.17$ and $k_x c/\omega = 1.007$. (a-i) Result obtained with CST Microwave Studio [55]. (a-ii) Result obtained with the effective medium model. (b-i) Similar to (a-i) but for the mode associated with the circular-shaped red symbol in Fig. 3(b) obtained with CST Microwave Studio [55]; the mode has $\omega a/c = 0.506$ and $k_x c/\omega = 1.005$. (b-ii) Transverse field profile for the same mode as in (a-i). The green dashed curves are calculated with the effective medium model and the blue solid curves with the full-wave simulator [55].

and the effective model slightly deteriorates near the interfaces [$z = 0$ and $z = 20a$, see Fig. 4(b-ii)] because of higher order evanescent waves not captured by the effective medium formalism.

The results of Fig. 4 confirm that the weakly bounded guided modes (with $k_x c/\omega \approx 1$) may exhibit a very fast variation along the z-direction. This is evident in the time snapshot of the TM field shown in Fig. 4(a-i) and (a-ii). Clearly, the longitudinal component of the wave vector is much smaller than the transverse component (i.e., $k_x/k_z \ll 1$), which is in agreement with the hyperbolic isofrequency contours of the bulk medium (see Fig. 2). For increasing frequencies, the discrepancy between the transverse and longitudinal wave numbers is progressively smaller [see Fig. 4(b-i)].

V. Detection of Structural Imperfections

The rather short transverse wavelength of the guided modes may be advantageously exploited to detect structural defects or imperfections with subwavelength dimensions in the host medium. For example, they may be used to detect

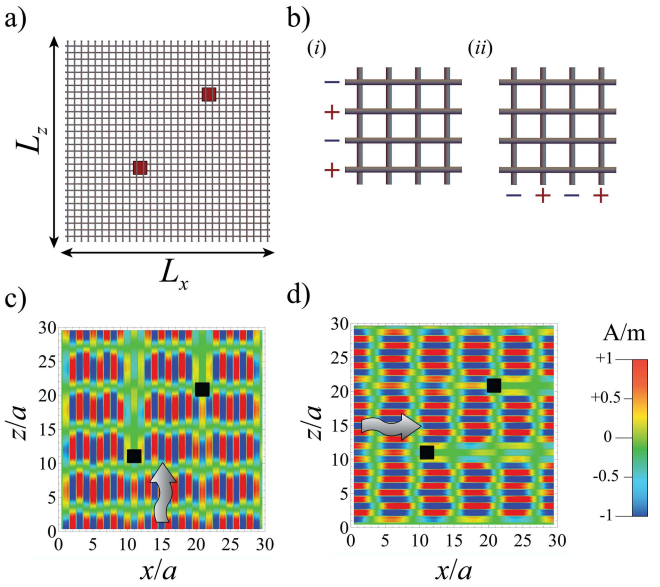

Fig. 5. (a) Geometry of a square wire grid with lattice period $a = L/30$ and wire radius $r_w = 0.05a$, with two square-shaped obstacles with dimensions $2a$ placed inside the grid. The obstacles are made of a highly absorbing material ($\varepsilon_{obs}/\varepsilon_0 = 1 - j5$, $\mu_{obs}/\mu_0 = 1 - j5$). (b) Illustration of the wire grid excitation. (c) and (d) Time snapshots of the normalized magnetic field $H_y(t = 0)$ obtained with CST Microwave Studio [55], for a wire grid with $a = 1$ mm and $f = 23.9$ GHz. (c) Excitation of the z-oriented wires. (d) Excitation of the x- oriented wires. The direction of the wave propagation is indicated by the gray arrows.

structural changes due to the exposure of the material to adverse conditions (e.g., high pressure, mechanical deformations, etc.), which may lead to cracks or other defects.

To illustrate the idea, we consider a scenario wherein a pair of subwavelength square-shaped obstacles (with dimensions $p_x = p_z = 2a$) made of a highly absorbing material is placed inside a square wire grid with dimensions $L_x = L_z = 30a$ and lattice constant $a = 1$ mm [see Fig. 5(a)]. A fast-varying guided mode is generated by exciting adjacent planes of metallic wires with voltages in opposition of phase, as illustrated in Fig. 5(b). The two orthogonal sets of wires are excited separately: first, the wires parallel to the z-direction [see Fig. 5(b-i)] and then the wires oriented along the x-direction [see Fig. 5(b-ii)].

In Fig. 5(c) and (d), we show time snapshots of the radiated magnetic field, $H_y(t = 0)$, in the presence of the two subwavelength absorbing obstacles, for each of the two excitations discussed previously and for the oscillation frequency $f = 23.9$ GHz. The results were obtained using CST Microwave Studio [55]. Notwithstanding the subwavelength dimensions of the absorbing obstacles, two prominent shadows are perfectly discernible behind the obstacles position. In this example, the shadow regions are due to the energy absorbed by the particles. The emergence of the subwavelength shadows is only possible due to the fast transverse variation of the guided modes supported by the wire grid. A similar effect would occur in the presence of a crack that disrupts some subset of metallic wires. Thus, the proposed structure may be useful to detect and localize defects due to structural changes of the host material.

VI. Conclusion

In conclusion, it was demonstrated that with the continuum approximation, a nonconnected crossed wire grid supports a diverging number of guided mode branches that pile up near the light line for low frequencies. In practice, due to the granularity of the metamaterial, the number of guided modes is finite and depends on the wire density. The comb-like structure of the dispersion diagram is rooted in the strong hyperbolic response of the double-wire array near the static limit. It was shown that even though the guided modes are weakly attached to the wire grid slab, they exhibit an extremely fast field variation along the transverse direction. Finally, it was suggested that the studied metamaterial may be useful to pinpoint subwavelength defects or imperfections due to structural changes of the host material.

References

[1] C. R. Simovski, P. A. Belov, A. V. Atrashchenko, and Y. S. Kivshar, "Wire metamaterials: Physics and applications," *Adv. Mater.*, vol. 24, no. 31, pp. 4229–4248, Aug. 2012.

[2] W. Rotman, "Plasma simulation by artificial dielectrics and parallel-plate media," *IRE Trans. Antennas Propag.*, vol. 10, no. 1, pp. 82–95, Jan. 1962.

[3] J. Brown, "Artificial dielectrics," in *Progress in Dielectrics*, vol. 2. Hoboken, NJ, USA: Wiley, 1960, pp. 195–225.

[4] J. B. Pendry, A. J. Holden, W. J. Stewart, and I. Youngs, "Extremely low frequency plasmons in metallic mesostructures," *Phys. Rev. Lett.*, vol. 76, no. 25, p. 4773, 1996.

[5] P. A. Belov *et al.*, "Strong spatial dispersion in wire media in the very large wavelength limit," *Phys. Rev. B, Condens. Matter*, vol. 67, Mar. 2003, Art. no. 113103.

[6] C. R. Simovski and P. A. Belov, "Low-frequency spatial dispersion in wire media," *Phys. Rev. E, Stat. Phys. Plasmas Fluids Relat. Interdiscip. Top.*, vol. 70, Oct. 2004, Art. no. 046616.

[7] I. S. Nefedov, A. J. Viitanen, and S. A. Tretyakov, "Propagating and evanescent modes in two-dimensional wire media," *Phys. Rev. E, Stat. Phys. Plasmas Fluids Relat. Interdiscip. Top.*, vol. 71, Apr. 2005, Art. no. 046612.

[8] M. G. Silveirinha and C. A. Fernandes, "Homogenization of 3-D-connected and nonconnected wire metamaterials," *IEE Trans. Microw. Theory Tech.*, vol. 53, no. 4, pp. 1418–1430, Apr. 2005.

[9] M. G. Silveirinha, "Nonlocal homogenization model for a periodic array of ϵ-negative rods," *Phys. Rev. E, Stat. Phys. Plasmas Fluids Relat. Interdiscip. Top.*, vol. 73, Apr. 2006, Art. no. 046612.

[10] M. G. Silveirinha, "Additional boundary condition for the wire medium," *IEEE Trans. Antennas Propag.*, vol. 54, no. 6, pp. 1766–1780, Jun. 2006.

[11] S. I. Malovski and M. G. Silveirinha, "Nonlocal permittivity from a quasistatic model for a class of wire media," *Phys. Rev. B, Condens. Matter*, vol. 80, Dec. 2009, Art. no. 245101.

[12] M. G. Silveirinha, C. A. Fernandes, and J. R. Costa, "Electromagnetic characterization of textured surfaces formed by metallic pins," *IEEE Trans. Antennas Propag.*, vol. 56, no. 2, pp. 405–415, Feb. 2008.

[13] S. I. Maslovski and M. G. Silveirinha, "Mimicking boyer's casimir repulsion with a nanowire material," *Phys. Rev. A, Gen. Phys.*, vol. 83, Feb. 2011, Art. no. 022508.

[14] D. E. Fernandes, S. I. Maslovski, and M. G. Silveirinha, "Cherenkov emission in a nanowire material," *Phys. Rev. B, Condens. Matter*, vol. 85, Apr. 2012, Art. no. 155107.

[15] A. N. Poddubny, P. A. Belov, and Y. S. Kivshar, "Purcell effect in wire metamaterials," *Phys. Rev. B, Condens. Matter*, vol. 87, Jan. 2013, Art. no. 035136.

[16] T. A. Morgado, S. I. Maslovski, and M. G. Silveirinha, "Ultrahigh Casimir interaction torque in nanowire systems," *Opt. Express*, vol. 21, no. 12, pp. 14943–14955, 2013.

[17] A. Poddubny, I. Iorsh, P. Belov, and Y. Kivshar, "Hyperbolic metamaterials," *Nature Photon.*, vol. 7, pp. 948–957, Dec. 2013.

[18] M. G. Silveirinha, "Anomalous refraction of light colors by a metamaterial prism," *Phys. Rev. Lett.*, vol. 102, May 2009, Art. no. 193903.

[19] T. A. Morgado, J. S. Marcos, J. T. Costa, J. R. Costa, C. A. Fernandes, and M. G. Silveirinha, "Reversed rainbow with a nonlocal metamaterial," *Appl. Phys. Lett.*, vol. 105, Dec. 2014, Art. no. 264101.

[20] P. A. Belov, Y. Hao, and S. Sudhakaran, "Subwavelength microwave imaging using an array of parallel conducting wires as a lens," *Phys. Rev. B, Condens. Matter*, vol. 73, Jan. 2006, Art. no. 033108.
[21] M. G. Silveirinha, P. A. Belov, and C. R. Simovski, "Subwavelength imaging at infrared frequencies using an array of metallic nanorods," *Phys. Rev. B, Condens. Matter*, vol. 75, Jan. 2007, Art. no. 035108.
[22] P. A. Belov *et al.*, "Transmission of images with subwavelength resolution to distances of several wavelengths in the microwave range," *Phys. Rev. B, Condens. Matter*, vol. 77, May 2008, Art. no. 193108.
[23] P. Ikonen, C. Simovski, and S. Tretyakov, "Magnification of subwavelength field distributions at microwave frequencies using a wire medium slab operating in the canalization regime," *Appl. Phys. Lett.*, vol. 91, Jul. 2007, Art. no. 104102.
[24] G. Shvets, S. Trendafilov, J. B. Pendry, and A. Sarychev, "Guiding, focusing, and sensing on the subwavelength scale using metallic wire arrays," *Phys. Rev. Lett.*, vol. 99, Aug. 2007, Art. no. 053903.
[25] T. A. Morgado and M. G. Silveirinha, "Transport of an arbitrary near-field component with an array of tilted wires," *New J. Phys.*, vol. 11, no. 8, Aug. 2009, Art. no. 083023.
[26] T. A. Morgado, J. S. Marcos, M. G. Silveirinha, and S. I. Maslovski, "Experimental verification of full reconstruction of the near-field with a metamaterial lens," *Appl. Phys. Lett.*, vol. 97, Oct. 2010, Art. no. 144102.
[27] M. G. Silveirinha and C. A. Fernandes, "Nonresonant structured material with extreme effective parameters," *Phys. Rev. B, Condens. Matter*, vol. 78, Jul. 2008, Art. no. 033108.
[28] M. G. Silveirinha, C. A. Fernandes, J. R. Costa, and C. R. Medeiros, "Experimental demonstration of a structured material with extreme effective parameters at microwaves," *Appl. Phys. Lett.*, vol. 93, Oct. 2008, Art. no. 174103.
[29] T. A. Morgado, J. S. Marcos, M. G. Silveirinha, and S. I. Maslovski, "Ultraconfined Interlaced Plasmons," *Phys. Rev. Lett.*, vol. 107, no. 6, Aug. 2011, Art. no. 063903.
[30] Y. Liu, G. Bartal, and X. Zhang, "All-angle negative refraction and imaging in a bulk medium made of metallic nanowires in the visible region," *Opt. Express*, vol. 16, no. 20, pp. 15439–15488, 2008.
[31] J. Yao *et al.*, "Optical negative refraction in bulk metamaterials of nanowires," *Science*, vol. 321, no. 5891, p. 930, Aug. 2008.
[32] M. G. Silveirinha, "Broadband negative refraction with a crossed wire mesh," *Phys. Rev. B, Condens. Matter*, vol. 79, Apr. 2009, Art. no. 153109.
[33] T. A. Morgado, J. S. Marcos, S. I. Maslovski, and M. G. Silveirinha, "Negative refraction and partial focusing with a crossed wire mesh: Physical insights and experimental verification," *Appl. Phys. Lett.*, vol. 101, Jul. 2012, Art. no. 021104.
[34] M. G. Silveirinha, C. A. Fernandes, and J. R. Costa, "Superlens made of a metamaterial with extreme effective parameters," *Phys. Rev. B, Condens. Matter*, vol. 78, Nov. 2008, Art. no. 195121.
[35] M. G. Silveirinha, C. R. Medeiros, C. A. Fernandes, and J. R. Costa, "Experimental verification of broadband superlensing using a metamaterial with an extreme index of refraction," *Phys. Rev. B, Condens. Matter*, vol. 81, Jan. 2010, Art. no. 033101.
[36] M. G. Silveirinha, "Artificial plasma formed by connected metallic wires at infrared frequencies," *Phys. Rev. B, Condens. Matter*, vol. 79, Jan. 2009, Art. no. 035118.
[37] F. Lemoult, G. Lerosey, J. Rosny, and M. Fink, "Resonant metalenses for breaking the diffraction barrier," *Phys. Rev. Lett.*, vol. 104, May 2010, Art. no. 203901.
[38] F. Lemoult, M. Fink, and G. Lerosey, "A polychromatic approach to far-field superlensing at visible wavelengths," *Nature Commun.*, vol. 3, p. 889, Jun. 2012.
[39] J. T. Costa and M. G. Silveirinha, "Achromatic lens based on a nanowire material with anomalous dispersion," *Opt. Express*, vol. 20, no. 13, pp. 13915–13922, 2012.
[40] S. I. Maslovski and M. G. Silveirinha, "Ultralong-range casimir-lifshitz forces mediated by nanowire materials," *Phys. Rev. A, Gen. Phys.*, vol. 82, Aug. 2010, Art. no. 022511.
[41] I. S. Nefedov and C. R. Simovski, "Giant radiation heat transfer through micron gaps," *Phys. Rev. B, Condens. Matter*, vol. 84, Nov. 2011, Art. no. 195459.
[42] S. Maslovski, S. Tretyakov, and P. Belov, "Wire media with negative effective permittivity: A quasi-static model," *Microw. Opt. Technol. Lett.*, vol. 35, no. 1, pp. 47–51, 2002.
[43] P. A. Belov and M. G. Silveirinha, "Resolution of subwavelength transmission devices formed by a wire medium," *Phys. Rev. E, Stat. Phys. Plasmas Fluids Relat. Interdiscip. Top.*, vol. 73, May 2006, Art. no. 056607.
[44] F. Lemoult, N. Kaina, M. Fink, and G. Lerosey, "Wave propagation control at the deep subwavelength scale in metamaterials," *Nature Phys.*, vol. 9, pp. 55–60, Nov. 2012.
[45] F. Lemoult, M. Fink, and G. Lerosey, "Revisiting the wire medium: An ideal resonant metalens," *Waves Random Complex Media*, vol. 21, no. 4, pp. 591–613, Oct. 2011.
[46] Y. Tyshetskiy, S. V. Vladimirov, A. E. Ageyskiy, I. I. Iorsh, A. Orlov, and P. Belov, "Guided modes in a spatially dispersive wire medium slab," *J. Opt. Soc. Amer. B*, vol. 31, no. 8, pp. 1753–1760, 2014.
[47] J. S. Brownless, B. C. P. Sturmberg, A. Argyros, B. T. Kuhlmey, and C. M. de Sterke, "Guided modes of a wire medium slab: Comparison of effective medium approaches with exact calculations," *Phys. Rev. B, Condens. Matter*, vol. 91, Apr. 2015, Art. no. 155427.
[48] P. A. Belov, R. Dubrovka, I. Iorsh, I. Yagupov, and Y. S. Kivshar, "Single-mode subwavelength waveguides with wire metamaterials," *Appl. Phys. Lett.*, vol. 103, Oct. 2013, Art. no. 161103.
[49] M. G. Silveirinha and C. A. Fernandes, "Homogenization of metamaterial surfaces and slabs: The crossed wire mesh canonical problem," *IEEE Trans. Antennas Propag.*, vol. 53, no. 1, pp. 59–69, Jan. 2005.
[50] M. G. Silveirinha and C. A. Fernandes, "Transverse-average field approach for the characterization of thin metamaterial slabs," *Phys. Rev. E, Stat. Phys. Plasmas Fluids Relat. Interdiscip. Top.*, vol. 75, Mar. 2007, Art. no. 036613.
[51] I. S. Nefedov, A. J. Viitanen, and S. A. Tretyakov, "Electromagnetic wave refraction at an interface of a double wire medium," *Phys. Rev. B, Condens. Matter*, vol. 72, Dec. 2005, Art. no. 245113.
[52] P. A. Belov, C. R. Simovski, and P. Ikonen, "Canalization of subwavelength images by electromagnetic crystals," *Phys. Rev. B, Condens. Matter*, vol. 71, May 2005, Art. no. 193105.
[53] M. G. Silveirinha, C. A. Fernandes, and J. R. Costa, "Additional boundary condition for a wire medium connected to a metallic surface," *New J. Phys.*, vol. 10, May 2008, Art. no. 053011.
[54] M. G. Silveirinha, "Additional boundary conditions for nonconnected wire media," *New J. Phys.*, vol. 11, Nov. 2009, Art. no. 113016.
[55] (2018). *CST Microwave Studio*. [Online]. Available: http://www.cst.com